ELSEVIER

Journal of Alloys and Compounds 253–254 (1997) 471–474

Journal of ALLOYS AND COMPOUNDS

Hydrogen diffusion in oxides formed on surfaces of zirconium alloys

D. Khatamian

AECL, Chalk River Laboratories, Stn. 82, Chalk River, ON K0J-1J0, Canada

Abstract

Transport of hydrogen through oxide layers formed on zirconium and its alloys has been the focus of recent studies associated with hydrogen uptake in nuclear reactor core components. Hydrogen discussion in oxides has been studied by hydrogen implantation and ^{15}N hydrogen depth-profiling techniques and the microstructure and micro-chemistry of the oxide layers as well as the underlying substrates have been characterized using a variety of techniques such as XPS, XRD, TEM, AEM, RS, NRA and RHEED. The studies show that micro-structure and micro-chemistry of the underlying alloy can affect the characteristics of the oxide, and, in turn, the transport of hydrogen through the oxide and into the underlying metal. In certain cases the oxide layer can be a homogeneous medium for hydrogen diffusion, but in most cases it is heterogeneous and may contain extremely fine interconnected cracks and pores undetected by conventional micro-analytical techniques. These studies show that minute amounts of impurities in the alloy can affect the diffusion rates in the oxide by several orders of magnitude.

Keywords: Hydrogen; Diffusion; Zr–Nb oxides; Zirconium alloys; CANDU

1. Introduction

Due to their low thermal neutron cross section and high resistance to corrosion, zirconium alloys have been the metals of choice for the core components of nuclear reactors such as fuel cladding, calandria tubes and pressure tubes. In the CANDU™ reactors [1] fuel cladding and the calandria tubes are made of Zircaloy-2 and -4 and the pressure tubes are made of Zr–2.5Nb (Zr–2.5 wt% Nb), a stronger alloy than either Zircaloy. While Zircaloy components consist of only α-Zr phase with some intermetallic inclusions, the Zr–2.5Nb pressure tubes consist of α-Zr grains surrounded with a β-Zr network of nominal composition Zr–20Nb (Zr–20 wt% Nb). Mechanical and corrosion properties of the Zr–2.5Nb pressure tubes are strongly dependent on the initial fabrication route and subsequent treatment of these tubes, due to the fact that the β-phase is meta-stable at temperatures below 900 K. Hydrogen uptake in both Zircaloy and Zr–2.5Nb components can lead to embrittlement and subsequent failure of the components. The oxide film, grown on the surface of the alloy, is the principal route for hydrogen diffusion into the alloy and can act as a protective layer against hydrogen uptake by the components.

Earlier measurements indicated that the diffusion rate of hydrogen in oxide films grown in air on the Zr–2.5Nb alloy is at least three orders of magnitude higher than in the films grown on pure zirconium [2]. Further hydrogen diffusion studies indicated that the Zr–2.5Nb and the Zr–1Nb oxides are heterogeneous and may contain interconnected pores or other fast diffusion paths such as unoxidized regions and that the oxides grown on β-phase Zr–20Nb may be non-porous and homogeneous [3,4]. To improve our understanding of the nature of hydrogen diffusion in the pressure tube oxides and to relate this understanding to the microstructure of the tube as a result of its prior treatment history, a systematic study of the diffusion of hydrogen in the oxides grown on β-annealed Zr–20Nb and Zr–15Nb, aged Zr–20Nb and single-phase Zircaloy-2 (α-Zr) specimens was initiated. The observations are reported here.

2. Experimental

Specimens of nominal size 10×15×1 mm were cut from the as-received sheets of Zr–15Nb and Zr–20Nb material. The Zircaloy-2 samples were sliced (~1 mm thick) from a 12 mm diameter rod. Specimens of Zr–15Nb and Zr–20Nb alloys were annealed at 1123 K to transform them to single-phase β-Zr [5]. XRD showed that both Zr–15Nb and Zr–20Nb specimens were single-phase β-Zr. The Zr–20Nb specimens were then divided into four sets and the sets were aged at 773 K for 50 min, 3, 10 and 100 h separately to transform them to (β-Zr_{enr}+ω), (α+β-Zr_{enr}+ω), (α+β-Zr_{enr} and (α-Zr+β-Zr_{enr}+β-Nb) states,

0925-8388/97/$17.00
PII S0925-8388(96)03068-X

respectively [6]. All the samples were abraded, electropolished and then oxidized in ~633 K to grow oxide layers of ~2 μm thickness. The oxide films were then implanted with hydrogen for diffusion measurements. The hydrogen concentration profiles of the specimens, before and after a diffusion anneal, were measured using the ^{15}N hydrogen profiling technique [7].

3. Results and discussion

3.1. Zr–20Nb specimens

The hydrogen concentration depth profiles in the oxides, measured prior to hydrogen implantation, are shown in Fig. 1a. The figure shows that the hydrogen levels in the oxide increase slightly as the aging period of the alloy increases to 3 and 10 h and that the increase is much larger in the case of the alloy aged for 100 h. The hydrogen concentration profiles measured after hydrogen implantation are given in Fig. 1b. Although the specimens were implanted simultaneously under identical conditions, they have retained different amounts of hydrogen. The specimen aged for 50 min has retained all the implanted hydrogen and has behaved in a way similar to the β-annealed Zr–20Nb specimens [4]. In the oxide layers grown on the alloys aged for 100 h or longer no hydrogen peak is discernible anymore and almost all the implanted hydrogen has diffused away during implantation. In such cases, some specimens were implanted at lower temperatures to retain the hydrogen in the implanted peak region for subsequent diffusion measurements.

Fig. 2 shows the hydrogen concentration profiles obtained from a sample aged for 50 min. These profiles show that after the diffusion anneal the peak has broadened. The area under the initial and the broadened peak are almost identical, indicating that during the annealing process no hydrogen has escaped from the oxide. The characteristics of these profiles are similar to those observed in the oxides of the β-annealed Zr–20Nb alloy [4]. To obtain the diffusion coefficient, the profiles were analyzed using a treatment described earlier [4]. In such a treatment the diffusion equation, $\delta C(X,t)/\delta t = D[\delta C(X,t)/\delta X^2)]$, is solved assuming an initial Gaussian distribution representing the as-implanted peak and the boundary conditions $C(0,t)=C(\infty,t)=0$. The only fitting parameter in the treatment is the diffusion coefficient, D. The best fit to the diffusion coefficients resulting from such analysis at different temperatures gives

$$D = 2.6 \times 10^{-6} \exp(-149916/RT)$$

where D, the diffusion coefficient, is given in $m^2\,s^{-1}$, T is in K and R is 8.314 $J\,mol^{-1}K^{-1}$. Fig. 3 shows the concentration profiles typical of those observed in the samples aged for 3 h and longer. These profiles, in contrast to the profiles shown in Fig. 2, show that after the diffusion anneal, although the peak height has decreased, the peak width has not changed. They indicate that the

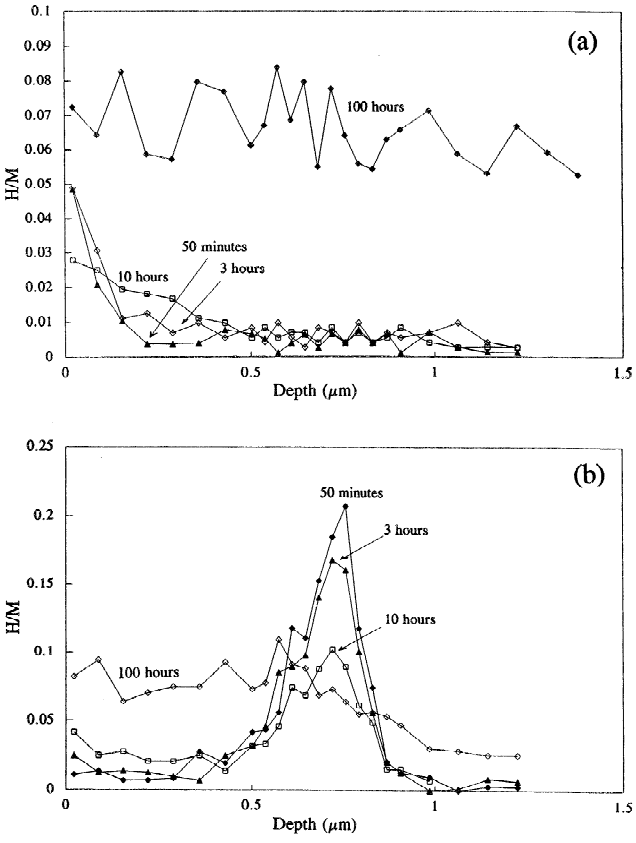

Fig. 1. Hydrogen concentration profiles of the water-grown oxide films on the Zr–20Nb samples annealed at 1123 K for 1 h and aged at 773 K for the specified periods, (a) before, and (b) after being implanted with hydrogen.

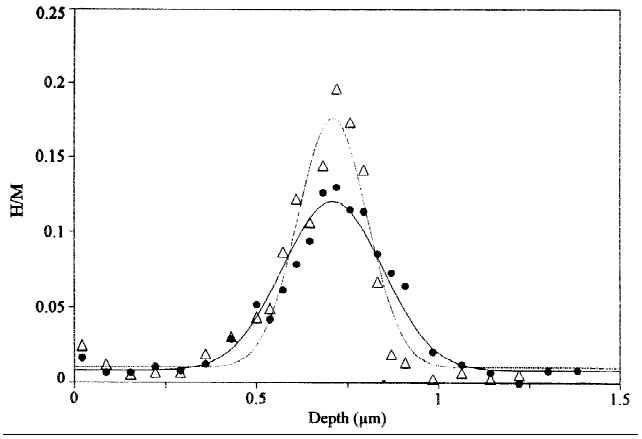

Fig. 2. Depth profiles for implanted hydrogen showing initial implantation (triangles) and after diffusion annealing for 21.5 min in 673 K air (circles). The oxide film was grown in 626 K water on the Zr–20Nb alloy aged for 50 min. The curves are the best Gaussian fits to the experimental points.

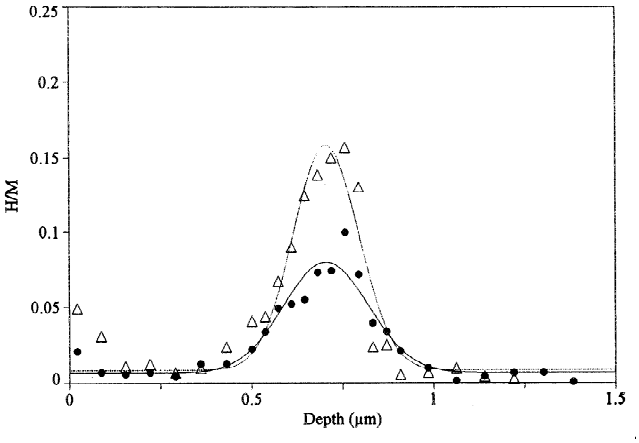

Fig. 3. Depth profiles for implanted hydrogen showing initial implantation (triangles) and after diffusion annealing for 4 min in 720 K air (circles). The oxide film was grown in 633 K water on the Zr–20Nb alloy aged for 3 h. The curves are the best Gaussian fits to the experimental points.

oxide has lost some of the implanted hydrogen. In this specific case the loss is ~30%. This behaviour has been attributed to a heterogeneous medium with short-circuit diffusion paths such as pores and/or unoxidized metallic regions. The profiles were analyzed using a previously developed simple model to be applied to the oxides with similar characteristics [2–4]. In this model the diffusion equation is solved with the width of the implanted peak kept constant. This condition imposes the restriction that the size of the homogeneous oxide cell (within the otherwise heterogeneous oxide layer) is equivalent to the width of the peak. The width of the implanted peak does not vary much between different oxides and is 0.4 μm. Therefore, in effect, the average size of the cells within all the oxides studied thus far is assumed to be ~0.4 μm. Of course, there is no experimental evidence or any other justification that the cell sizes in all these oxides are the same. In fact they may be very different even within a given sample. Since the derived diffusion coefficients depend on the cell size, the D values derived in this manner are not absolute and may only be used in comparison with other similarly obtained diffusion constants. The best fit to such relative and apparent diffusion coefficients, obtained at different temperatures, are given by the following Arrhenius equations:

$$D = 6.1 \times 10^{-9} \exp(-113804/RT);$$

Zr − 20Nb specimens aged for 3 h,

$$D = 4.5 \times 10^{-7} \exp(-129565/RT);$$

Zr − 20Nb specimens aged for 10 h,

$$D = 3.8 \times 10^{-11} \exp(-56003/RT);$$

Zr − 20Nb specimens aged for 100 h.

3.2. Zr–15Nb specimens

Initial profiles of the β-annealed Zr–15Nb samples showed hydrogen peaks very similar to the ones obtained from the β-annealed Zr–20Nb samples [4]. However, during diffusional anneal, unlike the results obtained from the Zr–20Nb samples, the hydrogen peak height had decreased with no changes in the peak width. To obtain apparent diffusion coefficients which can be compared with the previous results, the profiles were analyzed using the second diffusion model discussed above. As stated, the outcome of such analysis is not an absolute diffusion coefficient and it may only be used in comparison with others if similar diffusional behaviours are observed. The best fit to the apparent diffusion coefficients for the oxide of β-annealed Zr–15Nb gives

$$D = 1.99 \times 10^{-10} \exp(-89459/RT).$$

3.3. The Zircaloy-2 samples

The hydrogen profiles from the Zircaloy-2 specimens showed that diffusion annealing causes the hydrogen peak height to decrease with no change in the peak width. Also the as-implanted peaks indicated that some of the hydrogen escapes from the samples during implantation. These characteristics are very similar to the features discussed above in the case of the Zr–15Nb and Zr–2ONb specimens aged for more than 3 h. The second diffusion model was also used in this case to obtain some apparent diffusion coefficients for the Zircaloy-2 oxides. The best fit to the diffusion coefficients resulting from such analysis gives

$$D = 2.76 \times 10^{-9} \exp(-114841/RT).$$

4. Discussion

These results show that the oxides grown on Zr–20Nb alloy with β-Zr and β-Zr+ω phases constitute a homogeneous medium for hydrogen diffusion and as the traces of α-Zr appear within the alloy the character of the oxide changes and becomes heterogeneous. It is also evident that the hydrogen diffusion rates in the oxide increase with the increase in the amount of β-Nb present in the starting alloy. This is much more pronounced in the case of oxide films grown on the alloy aged for 100 h or more. The oxide may contain unoxidized or highly sub-stoichiometric regions to allow for the fast diffusion of hydrogen. Analysis using AEM as well as XPS have shown the presence of unoxidized niobium in such oxides [8,3]. In agreement with this, the oxides grown on pure Zr have very low diffusion rates for hydrogen [2] and provide much better protection against hydrogen ingress [9].

While the annealed Zr–15Nb samples have alloy microstructures and phase compositions identical to the annealed

Zr–20Nb samples, their oxides exhibit different characteristics with respect to hydrogen diffusion. Studies by XRD, Raman spectroscopy [10] and RHEED [11] have shown that the thin (~2 μm thick) oxide films grown on the annealed Zr–20Nb alloy have stabilized nearly-cubic-tetragonal (*nct*) (tetragonal with c/a very close to 1) crystal structure compared to the Zr–2.5Nb oxide, which is predominantly monoclinic. It seems that the 20 wt% Nb dissolved in Zr stabilizes the *nct* oxide, and thus prevents the allotropic transformation to the monoclinic structure. On the other hand, the amount of niobium in the Zr–15Nb (β-Zr) samples may not be enough to fully stabilize the oxide, or the alloy may contain small amounts of α-Zr, undetected by XRD, causing the formation of a heterogeneous mixed oxide structure. The transformation from the *nct* to the monoclinic structure requires a small volume change which may cause the formation of microcracks and pores in the resulting monoclinic structure. Recent TEM analysis in the cross section of the thin stabilized β-Zr oxides have shown an equiaxed grain structure [12] compared to the columnar structure found in the α-Zr oxides [13]. In the case of α-Zr oxides, the columnar structure may form as a result of the very thin *nct* layer, stabilized by the high compressive stress near the oxide/alloy interface, transforming to a more stable monoclinic phase. In any case, a study of the crystal structure and microstructure of the Zr–15Nb oxides in comparison with the Zr–20Nb and Zr–2.5Nb oxides may help in understanding these differences.

Although Zircaloy-2 has a α-Zr structure, similar to pure zirconium, the diffusivities for hydrogen in its oxides are at least three orders of magnitude higher than in the oxides of pure Zr. The grain boundaries of the oxide, in the case of Zircaloy-2, may contain unoxidized minor-phase particles such as iron, nickel and tin, and cause the higher diffusivities for hydrogen. This is plausible because of the fact that such minor-phase particles have much less affinity for oxygen than zirconium and are not readily oxidized in the presence of zirconium.

5. Conclusions

The diffusion of hydrogen in the oxides of annealed Zr–15 Nb, annealed and aged Zr–20Nb and Zircaloy-2 have been studied. The results show that the axides grown on Zr–20Nb with β-Zr + ω phase (annealed and aged for 50 min) are homogeneous and may have stabilized *nct* structure, much like the oxides grown on the annealed Zr–20Nb material. As the alloy ages and traces of α-Zr appear, the character of the oxide changes and becomes heterogeneous. The hydrogen diffusion rates in the oxide increase with the increase in the amount of β-Nb present in the starting alloy. This is much more evident in the case of oxides grown on the alloy aged for 100 h or more. The oxides grown on the annealed Zr–15Nb and Zircaloy-2 have, also, heterogeneous microstructures consisting of fast diffusion pathways for hydrogen.

Acknowledgments

The skilful efforts of V.C. Ling are very much appreciated for preparation of the specimens. Helpful discussions with V.F. Urbanic and his critical review of the report are acknowledged. The author also wishes to thank J.E. Winegar for obtaining XRD patterns of some of the specimens. The samples were implanted at the Cornell University Ion Implantation Facility and were analyzed for hydrogen depth profiles at the Accelerator Laboratory of McMaster University. This work was funded by COG WP #35 under WPIR #3182.

References

[1] C.E. Ells, *Canadian Metallurgical Society Annual Volume, 17* (1978) 32.
[2] D. Khatamian and F.D. Manchester, *J. Nucl. Mater., 166* (1989) 300.
[3] V.F. Urbanic et al., *ASTM-STP, 1245* (1994) 116.
[4] D. Khatamian, *Z. Phys. Chem., 181* (1993) 435.
[5] J.P. Abriata and J.C. Bolcich, *Bul. Alloy Phase Diagrams, 3* (1982) 1711.
[6] B.A. Cheadle and S.A. Aldridge, *J. Nucl. Mater., 47* (1973) 255.
[7] D. Khatamian, *J. Alloys and Compounds, 231* (1995) 722.
[8] Y.P. Lin, Ontario Hydro Technologies, Materials Unit, 800 Kipling Ave., Toronto., ON M8Z-5S4, Canada, unpublished results.
[9] M. Ellmoselhi, Ontario Hydro Technologies, Materials Unit, 800 Kipling Ave., Toronto, ON M8Z-5S4, Canada, unpublished results.
[10] O.T. Woo et al., *Proc. Mater. Res. Soc. Symp. 357, Boston, MA, USA, November 27–December 2 1994*, MRS 1995, p. 219; Y.P. Lin et al., *Proc. Mater. Res. Soc. Symp. 343, San Francisco, CA, USA, April 4–8 1994*, MRS 1994, p. 487.
[11] D. Khatamian and S.D. Lalonde, *J. Nucl. Mater.*, in press.
[12] O.T. Woo, Chalk River Laboratories, Chalk River, ON K0J-1J0, Canada, unpublished results.
[13] B.D. War et al., *ASTM-STP, 1132* (1991) 740.